Chemically Amplified Resist Fundamentals Studies by Combinatorial Approaches

Michael X. Wang, Vivek M. Prabhu, Eric K. Lin, Michael J. Fasolka, and Alamgir Karim

Polymers Division, National Institute of Standards and Technology, Gaithersburg, MD 20899

INTRODUCTION

The fabrication of sub-100 nm features via photolithography requires a detailed understanding of photoresist properties and processing conditions to achieve a fine control of the critical dimension (CD) and line-edge roughness (LER). Many photoresist material factors and process variables can impact both CD and LER, including segregation of the photoacid generator molecules or resist additives, photogenerated acid diffusion and acidolysis reaction, outgassing of photoresist materials, copolymer composition and phase separation between protected and deprotected polymers, photoacid generator (PAG) concentration, film thickness, exposure dose, post exposure bake times (PEB) and temperatures. Due to its complexity, it is not completely understood how these factors contribute to LER and CD. Integration of combinatorial techniques with traditional research and development approaches provides a powerful approach to rapidly conduct lithographic materials research.

The diffusion of photogenerated acid during PEB in the photoresist has been identified as a primary source of image blur and CD control [1]. In a typical positive-tone resist system, acid species generated by radiation and thermal diffusion during PEB can catalyze deprotection reaction of a large number of protection groups and make the resist soluble. The spatial extent of this deprotection reaction is known to be dependent on the system dimensions, i.e. film thickness and feature size. For example, it was reported that the glass transition temperature of ultrathin resist films can be dramatically different from its bulk property [2]. Associated thin film confinement effects on diffusion-reaction rate were observed in a model bilayer system recently by Goldfarb *et al*. [3].

In the work of Goldfarb *et al.*, a model bilayer system consisting of a protected bottom layer and deprotected top layer loaded with a PAG was used. The bilayer system emulates the interface between exposed and unexposed regions in a patterned photoresist. In this simplified approach, a flood exposure removes the contribution of the aerial image to the spatial distribution of acid in the resist. During PEB, the acid may diffuse into the protected layer creating an advancing front of deprotection. After development, changes in the thickness of the protected layer are used to identify the final position of the reaction boundary. By studying bilayer samples prepared under identical exposure and PEB conditions, observed changes are related to confinement-induced effects from either the substrate or the confinement itself. In this work, we follow this simple experimental scheme, but adopt high throughput methods to study PEB temperature and protected layer thickness effects by using temperature and thickness gradients, respectively.

EXPERIMENTAL

The deprotected polymer [poly(4-hydroxystyrene)] (PHS) with number average molecular weight of 19.0 kg/mol and the fully protected polymer [poly(tert-butoxycarboxystyrene)] (PBOCSt) with number average molecular weight of 15.3 kg/mol were prepared by free radical polymerization. Di(t-butylphenyl) iodonium perflurooctanesulfonate (PFOS) acid was obtained from DayChem. Propylene glycol methyl ether acetate (PGMEA), hexamethyldisilazane, toluene and 1-butanol were purchased from Aldrich and used without further purification. Developer CD-26 (tetramethyl-ammonium hydroxide (TMAH) 0.26 N) was obtained from Shipley [4].

Film thickness was measured using a Filmetrics F20 UV-visible interferometer with a spot of 1 mm diameter. The n and k dependences of wavelength were determined from a thick PBOCSt film (800 nm) using a Cauchy model. The reflectivity spectrum was then fit with thickness as the only variable. The film thickness calculated with this technique was also compared to the value obtained from x-ray reflectivity. Though the thickness obtained from the interferometer was generally 2 nm larger than that from x-ray reflectivity, thickness changes should be very close from two measurements. Here, only interferometeric data were used. Note the film was vacuum dried overnight before the thickness measurement. For a 100 nm film with about 1 % residual solvent, a floating index of refraction is needed to fit the spectrum and subsequently the thickness depends the initial fitting value. Film thickness standard uncertainty was within ± 1 nm. Roughness was measured via atomic force microscopy (DI 3000 AFM, Digital Instruments) in tapping mode using commercial software. The scan size was 5 μm $\times$ 5 μm. The root mean squared (RMS) roughness is calculated as the standard deviation of the height values within the measured area.

Samples consisted of bilayers of protected PBOCSt (bottom) and deprotected PHS (top) polymers on a hydrophobic silicon substrate. Thin <100> silicon wafers (Silicon, Inc.; (350 to 450) μm thick; 100 mm in diameter) were O_2 plasma cleaned to remove residual organic contaminants and treated with HF acid to remove the native silicon oxide surface. A controlled oxide layer was then regrown in a UV ozone chamber to a thickness of (10 to 20) Å. A hydrophobic surface was generated by priming the silicon wafers with hexamethyldisilazane vapor in a vacuum oven.

Two approaches were used to prepare the bottom PBOCSt layer for baking and thickness gradients, respectively. For the post applied bake study, the PBOCSt layer was spin cast from solution of PGMEA at 33 rad/s and subsequently baked at 110 ^{o}C for 60 s on a vacuum hot plate (1100 CEE, Cost Effective Equipment) and dried at 80 ^{o}C under vacuum before the film thickness was measured. For the thickness confinement study, the bottom layer was prepared by a custom-made "flow coater" [5]. This device consists of a doctor blade suspended over the specimen substrate mounted on a computer controlled motion stage. A small bead of PBOCSt solution (4.8 % by mass fraction in a 50:50 mixture of PGMEA and toluene) was inserted between the blade and the substrate. Subsequently, the stage was moved at constant acceleration to spread the solution. As the solvent evaporates a thickness gradient was formed along the direction of stage motion. Here, the solvent evaporation rate was adjusted such that the solution spread well without dewetting. To achieve this, the silicon wafer was heated to 105 ^{o}C during the flow coating process, and toluene was added to the solution mixture. After casting, the films were kept at 80 ^{o}C under vacuum overnight to remove residual solvent. Then, the film thickness was measured on a 2D grid every 2 mm.

The bilayer was completed by spin casting a PHS layer onto the PBOCSt film from a 1-butanol solution with (5 % PHS mass fraction and 5 % PFOS mass fraction relative to the mass of PHS). The bilayer was baked at 110 ^{o}C for 60 s. Next, the bilayer system was exposed to a broadband UV source (Oriel Instruments) with wavelengths from 220 nm to 260nm for a total dose of 500 mJ/cm^2. To remove post exposure delay effects, the PEB was carried out within 1 min. The single-thickness specimen was baked on a contact hotplate with a temperature gradient ranging from 70 ^{o}C to 140 ^{o}C for selected times, while the sample with a thickness gradient was baked at 110 ^{o}C on the vacuum hotplate for selected times.

After the PEB the bilayer films were developed by immersing the film in TMAH 0.26 N for 30 s, followed by a de-ionized water rinse. This removes the PHS top layer and the deprotected section of the PBOCSt bottom layer. After vacuum dried, the thickness of the remaining PBOCSt layer was remeasured in 2 mm increments over a 2D grid; while the roughness was measured from areas with different thickness and PEB time.

RESULTS and DISCUSSION

Figure 1 shows the reaction front profiles as a function of PEB temperature. For a sample without PEB, there is no observable thickness change, indicating the development effect on PBOCSt is negligible. For the baking samples, the loss of thickness increases as PEB temperature increases to about 110 ^{o}C and then becomes flat, which was also observed by traditional methods [3]. The reason for

this plateau is still unclear but it may be related to effects of proximity of PBOCSt Tg. It is clear that acid diffusion does not follow the Fickian model: the loss of thickness is not proportional to $t^{1/2}$. The possible reason is the poorly controlled environment, which may change the interface between PBOCSt and PHS. However, this method remains a powerful approach to rapidly prescreen the effects of PEB temperature and time on the reaction qualitatively.

The final developed samples were measured to obtain LER information as a function of PEB temperature and time by AFM. Our results showed a similar RMS of 1 nm for all the samples that went through deprotection and development. Note there is no observable roughness change from vacuum dry at 100 °C after development. The sample going through development but without deprotection process had a RMS of 0.4 nm, the similar roughness as the spin cast PBOCSt film.

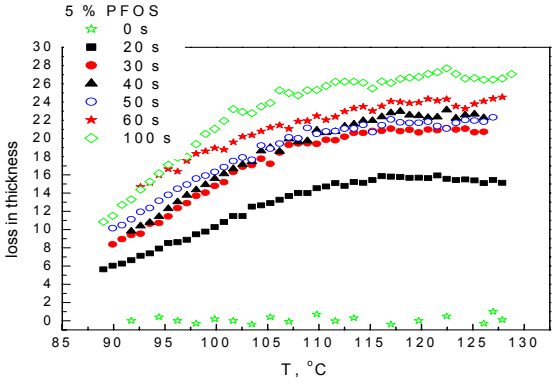

Figure 1. Plot of loss in thickness as a function of PEB temperature for different times.

Figure 2 shows representative 3D plots of PBOCSt layer thickness loss after the 60 s PEB and development. The original film has a thickness gradient from 40 nm to 130 nm. The plateau, where the original thickness is above (60 ± 5) nm, shows no thickness dependence. The fact that the Δd decreases with decreasing original thickness of PBOCSt layer below (60 ± 5) nm suggests that the thin film confinement has dramatically slowed down the reaction-diffusion rate.

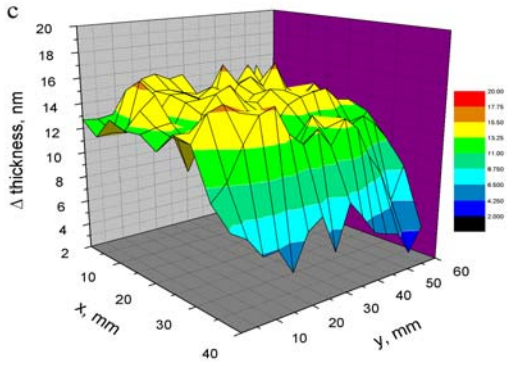

Figure 2. 3D Plot of PBOCSt loss in thickness.

In order to quantify the thickness effects on the reaction-diffusion rate, the final thickness changes were averaged over the points with same original film thickness (1 nm bin). The statistical error is less than 1.5 nm. Figure 3 shows thickness changes of the PBOCSt layer as a function of the PEB time for different film thickness. For all thicknesses, the Δd increases with PEB time below 60 s, while there is

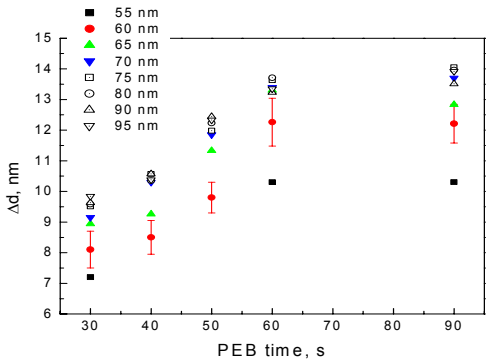

Figure 3. Thickness change of PBOCSt layer as a function of PEB times for different film thickness. The related standard uncertainty are similar for each data point and were only shown for 60 nm as an example.

no difference between 60 s and 90 s. The time dependence of Δd does not exactly follow a Fickian equation as Goldfarb *et al.* reported [3]. One possible reason is that we did not maintain identical processing conditions for each wafer resulting in apparent changes in the reaction-diffusion rate. The almost equivalent Δd after 60 s and 90 s PEB times indicates that the deprotection reaction has stopped after 60 s under current processing conditions. This may be due to acid trapping or neutralization via base molecules from environment contamination. Nevertheless, because the process conditions are identical within a thickness gradient specimen, the thickness dependence of Δd shows very similar behavior for different PEB times. Indeed, this "processing consistency" is an extra advantage of using these combinatorial methods. The AFM roughness measurements for all samples gives same R_{ms} (1.2 ± 0.1) nm, showing no thin film confinement effects, indicating that the LER will be similar for all thickness.

* Contribution of NIST, not subject to copyright in the USA.

ACKNOWLEDGEMENTS

This work was partially supported by the Defense Advanced Research Projects Agency Advanced Lithography Program under grant N66001-00-C-8083 as well as by the NIST Combinatorial Methods Center. We thank IBM for providing the PHS and PBOCSt materials used in this study.

REFERENCS AND NOTES

1. Houle, F. A., Hinsberg, W. D., Morrison, M., Sanchez, M. I., Wallraff, G.,Larson, C., and Hoffnagle, J. *J. Vac. Sci. Technol.* **2000**, B18, 1874.
2. Fryer, D. S. Nealey, P. F., and de. Pablo, J. *Macromolecules* **2000**, 33, 6439.
3. Goldfarb, D. L., Angelopoulos, M., Lin, E. K., Jones, R. L., Soles, C. L., Lenhart, J. L., and Wu, W. *J. Vac. Sci. Technol.* **2001**, B19, 2699.
4. Commercial equipment and materials are identified in this proceeding only to adequately specify experimental procedure In no case does this imply endorsement or recommendation by the National Institute of Standards and Technology.
5. Meredith, J. C., Smith, A. P., Karim, A., and Amis, E. J. *Macromolecules* **2000**, 33, 9747.